

## Compact fibre-based coherent anti-Stokes Raman scattering spectroscopy and interferometric coherent anti-Stokes Raman scattering from a single femtosecond fibre-laser oscillator

VIKAS KUMAR\*, ALESSIO GAMBETTA, CRISTIAN MANZONI, ROBERTA RAMPONI, GIULIO CERULLO and MARCO MARANGONI  
Dipartimento di Fisica-Politecnico di Milano, ULTRAS-CNR-INFM, IFN-CNR,  
Piazza Leonardo da Vinci 32, 20133 Milano, Italy

\*Corresponding author. E-mail: nasavikas@gmail.com

**Abstract.** We demonstrate a new approach to CARS spectroscopy by efficiently synthesizing synchronized narrow-bandwidth (less than  $10\text{ cm}^{-1}$ ) pump and Stokes pulses (frequency difference continuously tunable upto  $\sim 3000\text{ cm}^{-1}$ ) based on spectral compression together with second harmonic generation (in periodically-poled nonlinear crystals) of femtosecond pulses emitted by a single compact Er-fibre oscillator. For a far better signal to non-resonant background contrast, interferometric CARS (I-CARS) is demonstrated and CARS signal enhancement upto three orders of magnitude is achieved by constructive interference with an auxiliary local oscillator at anti-Stokes field, also synthesized by spectral compression of pulses emitted from the same fibre oscillator.

**Keywords.** Coherent anti-Stokes Raman scattering; nonlinear spectroscopy; coherent spectroscopy; interferometric CARS.

**PACS Nos** 42.65.Dr; 78.47.N; 78.47.jh

The coherent anti-Stokes Raman scattering (CARS) is a label-free high-sensitivity nonlinear spectroscopy technique that is capable of real-time non-invasive biomedical video-rate imaging based on molecular vibrational spectroscopy offering intrinsic chemical selectivity [1]. The nonlinear nature of the CARS process automatically grants it the capability of three-dimensional sectioning which is essential for imaging thick samples. In CARS process, two temporally and spatially overlapped narrow-band pulses, pump frequency,  $\omega_p$ , and Stokes frequency,  $\omega_s$ , interact with a sample via a wave-fixing process. When beat frequency  $\Omega = \omega_p - \omega_s$  is tuned to Raman-active molecular vibration of the sample molecule, the resonant oscillators within the sample are coherently driven by the excitation fields, thereby generating a strong anti-Stokes signal at  $\omega_{as} = 2\omega_p - \omega_s$  representing a unique chemical signature of the resonant oscillator molecule.

CARS spectroscopy requires two synchronized pulse trains with narrow bandwidth (a few  $\text{cm}^{-1}$ ; vibrational linewidths are typically of the order of  $10\text{--}20\text{ cm}^{-1}$ )

and independent tunability over a wide spectral range (800–3300  $\text{cm}^{-1}$ ), which presently use biomedical application set-ups achieved either by a pair of electronically locked picoseconds Ti:sapphire oscillators [2] or by an optically parametric oscillator [3,4]. Both excitation set-ups are complex and bulky. One serious problem of CARS spectroscopy is the presence of strong non-resonant background due to four-wave mixing process (independent of the Raman shift). This background being coherent, interferes with CARS signal, can distort it and even bury it if it is generated from low concentration of Raman-active molecules. Two techniques have been demonstrated to improve signal to background contrast so far: frequency modulation CARS (FM-CARS) [5,6] for background suppression which needs generation of second synchronized pump/Stokes field at a slightly different frequency and interferometric CARS (I-CARS) [7–9] which gives CARS signal enhancement, exploiting interference of CARS field with another field (local oscillator, LO) at anti-Stokes frequency phase coherent with pump and Stokes fields for homodyne detection. Thus these techniques require an additional third colour synchronized (also phase coherent in the case of I-CARS) with pump/Stokes.

In this work, we demonstrate a new approach towards the much compact set-up for CARS spectroscopy/microscopy, in which multiple (pump, Stokes and LO) continuously tunable narrow-band phase-coherent pulses are synthesized by spectral compression of femtosecond pulses emitted by a single highly compact fibre laser. Spectral compression of the broadband femtosecond pulses is achieved by generating narrow-band second harmonic (SH) pulses in crystals with large group-delay mismatch between the fundamental frequency (FF) and the SH pulses [10,11]. Such a technique was recently demonstrated by our group [11,12]. When applied to CARS in combination with fibre-format sources, it allows a dramatic improvement of the set-up in terms of compactness, simplicity and, most of all, versatility, thanks to the possibility of easily synthesizing a third phase-coherent colour to be applied either for FM-CARS or for I-CARS techniques.

The experimental set-up is shown in figure 1. The laser source is a commercial 100 MHz Er-doped fibre oscillator with two fibre amplified branches (Toptica FFS model), each one delivering nearly 70 fs long pulses at 1550 nm with 2.5 nJ energy, resulting in a 250 mW average power. One of the outputs is coupled to a highly nonlinear fibre producing an octave-spanning supercontinuum (SC) from 1000 to 2200 nm. The SC consists of two well distinct bands at opposite positions with respect to the 1550 nm wavelength, each one exhibiting a main spectral peak whose position can be easily tuned by changing the chirp of the pulses entering the nonlinear fibre. Figure 2 shows, as dashed lines, the spectrum of the 1550 nm output and a sequence of spectra of the long-wavelength peak of the SC, tunable from 1700 to 2000 nm. The 1550 nm output and the SC, derived from the same laser oscillator, are phase-coherent. The 1550 nm pulse train is spectrally compressed by tight focussing in a 18-mm long periodically poled lithium niobate (PPLN) crystal to produce narrow-band ( $<10 \text{ cm}^{-1}$ ) pump pulses at 775 nm with up to 40 mW average power (solid line in the figure). The long-wavelength peak of the SC is compressed in a 20-mm PPLN crystal equipped with multiple poling periods, so as to generate narrow-band ( $<15 \text{ cm}^{-1}$ ) Stokes pulses with 1–4 mW power and tunability from 800 to 1050 nm, corresponding to a frequency difference between pump and Stokes pulses ranging between 1000 and 3300  $\text{cm}^{-1}$  (see figure 2). Both

Single femtosecond fibre-laser oscillator

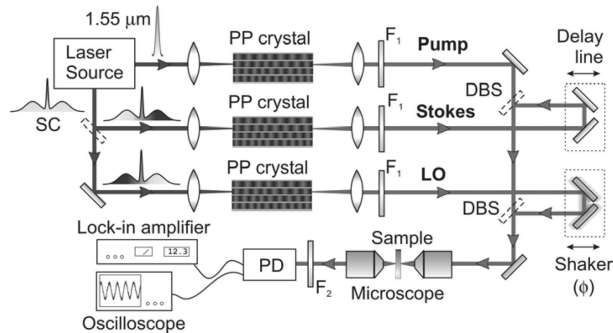


**Figure 1.** Experimental set-up. DBS: dichroic beam splitter; F1: band-pass filter; F2: short/band-pass filters; PP: periodically-poled crystals; SC: supercontinuum; PD: photodetector.

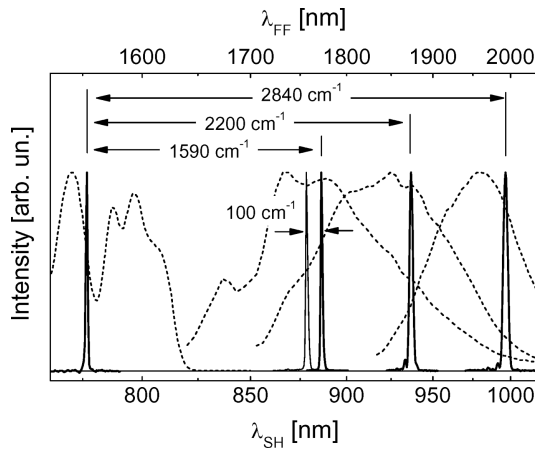


**Figure 2.** Compressed SH spectra (solid lines, bottom scale) and the corresponding FF spectra (dashed lines, top scale).

PPLN crystals are mounted in ovens to allow for fine-frequency tuning ( $\sim 15 \text{ cm}^{-1}$  for a temperature change of  $10^\circ\text{C}$ ). The use of periodically-poled crystals for spectral compression is crucial because of the large nonlinear coefficient, allowing for high SHG efficiency and the large group-velocity mismatch between FF and SH, allowing for high spectral compression ratios. Pump and Stokes are synchronized by a delay line, combined by a dichroic beam splitter and focussed on the sample by a microscope objective. Then, a set of short-pass and band-pass filters selects the forward CARS signal, with a rejection of  $10^{13}$  on the pump and Stokes beams.

We tested our system in a solution of dimethyl sulphoxide (DMSO). Figure 3 shows the CARS intensity as a function of the frequency difference  $\omega_p - \omega_s$  when varied from  $2800$  to  $3000 \text{ cm}^{-1}$  by temperature and poling-period tuning. We observed the typical asymmetric dispersive shape of the CARS response, with a strong peak at  $2890 \text{ cm}^{-1}$  and a less intense one at  $2972 \text{ cm}^{-1}$ . The narrow width of the main peak ( $15.5 \text{ cm}^{-1}$ ) gives proof of the high spectral resolution of the

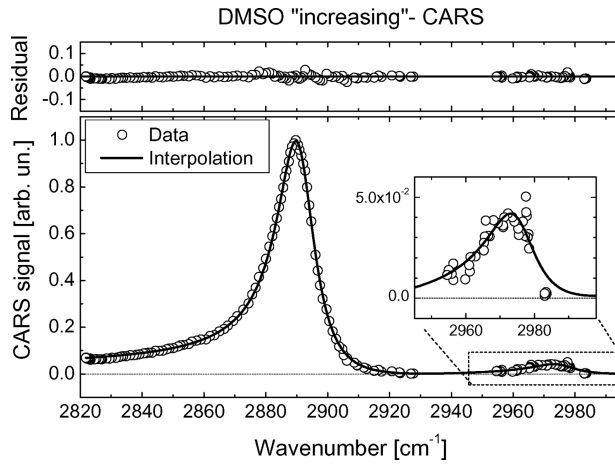


**Figure 3.** CARS signal as a function of the frequency detuning between pump and Stokes for DMSO solution.

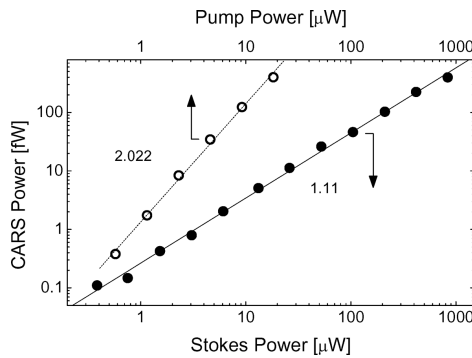


**Figure 4.** CARS power at the peak of the DMSO response as a function of pump and Stokes powers.

apparatus. The solid line in figure 3 shows a fit to the measured CARS signal using the response  $I_{\text{CARS}}(\Omega) \propto |\chi_{\text{R}}^{(3)}(\Omega) + \chi_{\text{NR}}^{(3)}|^2$  where  $\chi_{\text{R}}^{(3)}(\Omega)$  is the resonant CARS signal, consisting of two Lorentzian resonances, and  $\chi_{\text{NR}}^{(3)}$  is the non-resonant background. Figure 4 shows the dependence of the CARS signal on the average pump and Stokes powers: by using a bilogarithmic scale the experimental data are well fitted by linear fitting curves with 2.02 and 1.11 slopes for pump and Stokes respectively, which is consistent with the expected quadratic and linear dependences.

The above results demonstrate the feasibility of a fibre-format laser system for CARS microscopy. For the implementation of I-CARS, it is straightforward to generate a third narrow-band phase-coherent pulse at the anti-Stokes frequency to be used as a local oscillator. We tested for I-CARS by introducing in the Stokes branch a dichroic beam-splitter reflecting the short-wavelength part of the SC and

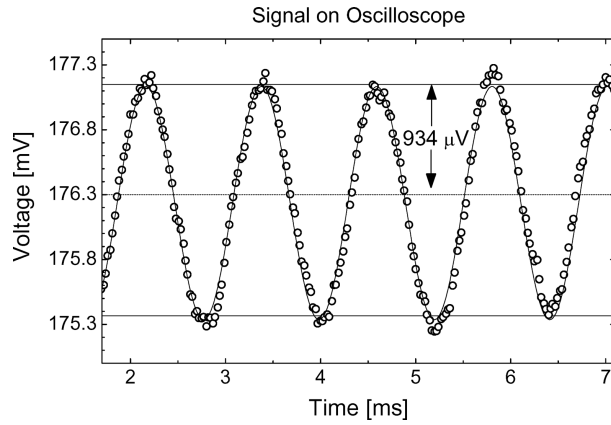


**Figure 5.** Interference pattern between CARS and LO as a function of their delay.

sending it to a third PPLN crystal for the synthesis of the narrow-band pulse at  $\omega_{\text{as}}$ . There is inherent phase-coherence among pump, Stokes and anti-Stokes pulses, which is ensured by the common driving laser oscillator, the anti-Stokes field when temporally and spatially overlapped with the other two fields, can be used as LO for homodyne amplification of the CARS signal, according to the well-known interference formula

$$P = P_{\text{CARS}} + P_{\text{LO}} + 2\sqrt{P_{\text{CARS}}P_{\text{LO}}}\cos\Delta\phi, \quad (1)$$

where  $\Delta\phi$  is the phase difference between LO and CARS signals. As a first phase-coherence test, we tuned to the peak of the DMSO response, attenuated the LO beam to the same power level of the CARS signal ( $\approx 1$  pW), and sent both signals to a spectrometer. According to the value of  $\Delta\phi$  a constructive interference up to  $3.7P_{\text{CARS}}$  (and destructive down to  $0.3P_{\text{CARS}}$ ) was observed. This gives experimental evidence of the phase coherence between CARS and LO beams, the only limitation coming from imperfect temporal and spatial matching. As a second step we increased the LO power to the  $\mu\text{W}$  level and detected with a photodiode the beating signal resulting from periodic modulation of  $\Delta\phi$ , as achieved using a shaker on the LO beam path. This allows to visualize the interference term in eq. (1) and obtain an amplification of the CARS signal by a factor of  $2\sqrt{P_{\text{LO}}/P_{\text{CARS}}}$ , as high as 2000 for an LO power of  $1 \mu\text{W}$ . Figure 5 shows the interference pattern acquired with an oscilloscope for an LO power of  $50$  nW: the modulation depth with respect to the continuous level given by the LO is  $\pm 0.5\%$ , which is consistent with the expected optical power ratio ( $\pm 250$  pW over  $50$  nW) given by eq. (1). Figure 6 shows as dots the amplitude of the homodyne interference term as a function of the LO power; a power-law fit (dashed line) yields a slope of  $0.49$ , in agreement with the expected square root dependence.

In conclusion, we have presented a new concept for generating tunable, synchronized narrow-band pulses starting from a single fibre-format femtosecond oscillator, which promises a dramatic simplification of the architecture of the driving laser for coherent vibrational microscopy. Finally, the capability of synthesizing

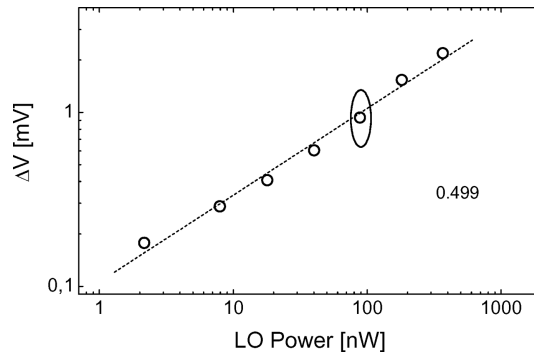


**Figure 6.** Modulation amplitude ( $\Delta V$ ) as a function of LO power.

additional phase-coherent multicolour pulses opens a host of opportunities for enhancing the CARS response, by coherent amplification and/or by non-resonant background suppression.

## References

- [1] C L Evans and X S Xie, *Annu. Rev. Anal. Chem.* **1**, 883 (2008)
- [2] E O Potma, D J Jones, J-X Cheng, X S Xie and J Ye, *Opt. Lett.* **27**, 1163 (2002)
- [3] C L Evans, E O Potma, M Puoris'haag, D Cote, C P Lin and X S Xie, *Proc. Natl. Acad. Sci. USA* **102**, 16807 (2005)
- [4] F Ganikhanov, S Carrasco, X S Xie, M Katz, W Seitz and D Kopf, *Opt. Lett.* **31**, 1292 (2006)
- [5] F Ganikhanov, C L Evans, B G Saar and X S Xie, *Opt. Lett.* **31**, 1872 (2006)
- [6] Y S Yoo, D-H Lee and H Cho, *Opt. Lett.* **32**, 3254 (2007)
- [7] E O Potma, C L Evans and X S Xie, *Opt. Lett.* **31**, 241 (2006)
- [8] B von Vacano, T Buckup and M Motzkus, *Opt. Lett.* **31**, 2495 (2006)
- [9] M Jurna, J P Korterik, C Otto, J L Herek and H L Offerhaus, *Opt. Express* **16**, 15863 (2008)
- [10] K Moutzouris, F Adler, F Sotier, D Träutlein and A Leitenstorfer, *Opt. Lett.* **31**, 1148 (2006)
- [11] M A Marangoni, D Brida, M Quintavalle, G Cirimi, F M Pigozzo, C Manzoni, F Baronio, A D Capobianco and G Cerullo, *Opt. Express* **15**, 8884 (2007)
- [12] M Marangoni, D Brida, M Conforti, A D Capobianco, C Manzoni, F Baronio, G F Nalesso, C De Angelis, R Ramponi and G Cerullo, *Opt. Lett.* **34**, 241 (2009)